Turkish Journal of Chemistry

http://journals.tubitak.gov.tr/chem/

Research Article

Turk J Chem
(2019) 43: 1472 – 1485

doi:10.3906/kim-1905-26

Synthesis and characterization of novel mussel-inspired benzoxazines by thiol-benzoxazine chemistry

Mustafa ARSLAN*
Department of Chemistry, Faculty of Arts and Sciences, Kırklareli University, Kırklareli, Turkey

Received: 13.05.2019 • **Accepted/Published Online:** 16.09.2019 • **Final Version:** 07.10.2019

Abstract: A catechol-based benzoxazine copolymer is reported via a new approach using an oxazine-thiol reaction. The main chain benzoxazine precursor was obtained via the classic benzoxazine synthesis methodology using the raw chemicals catechol, formaldehyde, and 4,7,10-trioxa-1,13-tridecanediamine. The countercomponent was synthesized from poly(ethylene glycol) methyl ether via the Fischer esterification reaction. The obtained reactive catechol-based benzoxazine was then reacted in mild conditions with polymeric thiol precursor to obtain a copolymer structure. The precursors and the resulting structure were characterized by thermal and spectral analyses using DSC, TGA, FT-IR, ^{1}H NMR, and GPC. Film formation was also demonstrated with unreacted oxazine ring units in the copolymer, and the ring opening polymerization temperature was lower than that corresponding to the benzoxazine precursor.

Key words: Polybenzoxazines, ring-opening polymerization, catechol, thiol-benzoxazine reaction

1. Introduction

Epoxies, phenolics, cyanate esters, bismaleimides, vinyl esters, and polyimides are the most commonly known thermosetting resin systems. Recently, polybenzoxazines (PBZs) have been introduced as a new type of these structures and attracted much attention. PBZs may be synthesized by thermally triggered ring-opening polymerization. Monomers or polymeric precursors of benzoxazines can form PBZs and they do not need any initiator, catalyst, or curative during the synthesis process. Nevertheless, catalysts or curatives should be added to reduce the ring-opening polymerization temperature of monomers. Their outstanding characteristics, including good char yield, noncatalytic synthesis, low shrinkage, high glass transition temperatures, and limited side product formation, make these polyphenolic thermosets attractive in different industrial and scientific fields such as structural materials, aerospace, adhesives, electronic applications, and paints [1]. The advantageous properties of PBZs are mostly due to hydrogen bond interactions of nitrogen and phenolic hydroxyl groups and CH_2–N(R)–CH_2 Mannich base bridges. Commonly, a cationic ring-opening mechanism was observed during the PBZ synthesis process with thermal treatment at around 200 °C (Scheme 1) [2].

The huge molecular diversity of the monomer components provides great convenience to synthesize novel monomers for various purposes [3–5]. Any appropriate phenol, primary amine, or formaldehyde may be used to obtain functional benzoxazine monomers with various properties [6–9]. Furthermore, PBZs with bio-based compounds support reduction of several challenges in toxicity and renewability of these polymeric materials. Various bio-based benzoxazines have been reported in low-cost phenolics [10,11] and amines including vanillin

*Correspondence: marslan@klu.edu.tr

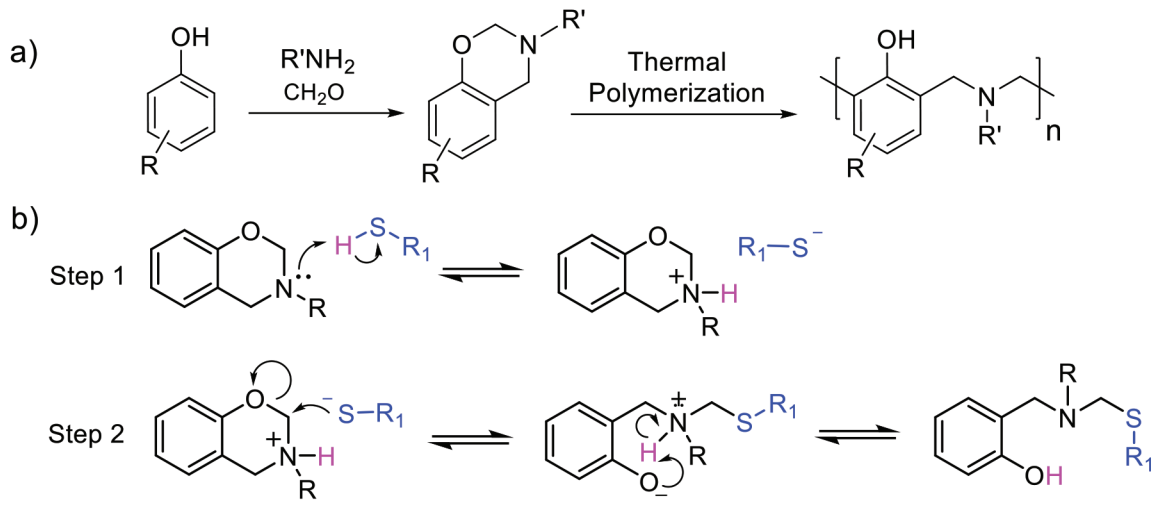

Scheme 1. Synthetic route to 1,3-benzoxazines and PBZs by ring-opening polymerization (ROP) (a) and plausible catalytic ring-opening mechanism of benzoxazines by thiols (b).

[12,13], cardanol [14,15], resorcinol [16], eugenol [17], catechol [18], urushiol [19], stearyl amine [20], guaiacol [20,21], furfuryl amine [22–24], chavicol [25], and gallic acid [26].

The high curing temperature of benzoxazines is an industrial and academic problem restricting the processability and application of the corresponding resin. Several research groups have investigated the mechanism of the catalytic ring-opening of 1,3-benzoxazines by thiols at room temperature. The approach was expressed as "Catalytic Opening of the Lateral Benzoxazine Rings by Thiols" (COLBERT) [27,28]. The COLBERT process is a two-step reaction [29] that proceeds over protonated ionic benzoxazine intermediate formation by thiol. Secondly, the attack of thiolates on the methyl carbon of the oxazine ring located between nitrogen and oxygen atoms occurs and forms ring-opened benzoxazine structures (Scheme 1). The COLBERT reaction is a reversible process following continuous regeneration of the thiol in the intermediate product. It was shown that the solvent system used affects the reversibility of the reaction. A novel polyaddition strategy based on addition of nucleophiles to obtain a linear benzoxazine was developed by Endo [30]. Yagci et al. obtained thermally curable benzoxazine networks. COLBERT and photoinduced thiol-ene reactions were simultaneously utilized [31]. A photoinitiator was used to trigger thiol-ene reactions and simultaneously the COLBERT reaction was generated by thiol compounds present in the reaction mixture. Another synthetic approach concerning the thiol-oxazine reaction is reported to obtain copolymer from a main-chain PBZ precursor. By selecting the appropriate benzoxazine structure and thiols, desired architectures can be produced for various applications in fast and easy conditions [32]. It was also demonstrated that block copolymers can be prepared by means of successive COLBERT procedures in sequence and one-pot synthesis, and this was suggested as novel thiol-X chemistry [33,34].

Recently, various research groups have focused on discovering catechol-including materials. The robust bioadhesive capacity of catechol-based structures provides strong adhesion under extreme conditions [35]. A functionalized amino acid, 3,4-dihydroxy-L-phenylalanine, comprises the catechol group as a crucial constituent used by mussels, which are marine organisms and crucial suppliers of the strong adhesion properties of plaque proteins [36]. Catechol must be combined with the appropriate polymer containing an optimal chain mobility, crosslink density, and mechanical property to benefit from its superior properties. It is necessary to integrate catechol with a well-defined polymer for advanced adhesive performance [37]. Various mussel mimetic polymers

were explored in polyamides [38], polypeptides [39], polyethylene glycols [40,41], polyacrylates [42,43], and polystyrenes [44]. Studies have found a variety of application areas including elastomers [45], hydrogels [46], nanoparticle shells [47], surface treatments [48], antifouling coatings, and antibacterial coatings [49].

As mentioned above, to benefit from mainly the COLBERT process and benzoxazine chemistry, polymeric benzoxazine precursors may be used as components of copolymers. The cured main-chain catechol-benzoxazine polymer (PCTBz) has a very stiff structure based on the classic flexible PBZ film, such that the main-chain catechol-benzoxazine (CTBz) polymer should be combined with the appropriate polymer precursor with an optimal chain mobility and mechanical property to benefit from its superior properties. The present study aimed to apply thiol-X chemistry for preparing a flexible bio-based benzoxazine film. The strategy was based on the COLBERT reaction, which was facilitated between the oxazine ring of benzoxazine and the thiol atoms of the polymer component. Likewise, to maintain interest in using a bio-based monomer, catechol could be used as a naturally existing structure, and firstly catechol-based main-chain type benzoxazines would be obtained. Thus, catechol, formaldehyde, and 4,7,10-trioxa-1,13-tridecanediamine (TTDDA) were chosen as the starting chemicals to obtain bio-based polymeric benzoxazine precursors, and the COLBERT reaction with thiol-modified poly(ethylene glycol) methyl ether was particularly examined.

2. Experimental

2.1. Materials

Catechol (1,2-dihydroxybenzene) (Aldrich, $\geq$99%), paraformaldehyde (Acros, 96%), 3-mercaptopropionic acid (Merck, $>$99%), 4,7,10-trioxa-1,13-tridecanediamine (Aldrich, $\geq$98%), poly(ethylene glycol) methyl ether (mPEG) (M_n: 2000 g mol^{-1}, Aldrich), sodium bicarbonate (Aldrich, $\geq$99.5%), chloroform (Acros, 99+%), diethyl ether (Merck, $\geq$98%), magnesium sulfate anhydrous (Aldrich, $\geq$99.5%), hexane (Merck, 95%), methanol (Merck, $\geq$99.8%), toluene (Aldrich, $\geq$99.5%), dichloromethane (Merck, CH_2Cl_2, $\geq$99.8%), deuterium oxide (Aldrich, D_2O, 99.9 atom% D), dimethyl sulfoxide-deuterated (Merck, DMSO-d_6, 99.9 atom% D), chloroform-d (Aldrich, $CDCl_3$), 99.8 atom% D), N,N-dimethylformamide (DMF, Sigma-Aldrich), and tetrahydrofuran (THF, Merck, 99.7%).

2.2. Measurements

The nuclear magnetic resonance (^{1}H NMR) analyses of the starting compounds and polymeric precursors were recorded in $CDCl_3$ or DMSO-d_6 by a 500 MHz Agilent NMR system (VNMRS). $Si(CH_3)_4$ was used as an internal standard. Thermogravimetric properties were investigated by a Setaram Sensys Evo TG-DSC instrument. The measurements were achieved from 30 to 900 °C with a 10 °C min^{-1} heating rate and under N_2. The Fourier transform infrared (FT-IR) spectroscopy measurements of the monomer and polymers were analyzed by a PerkinElmer FT-IR Spectrum One spectrometer. Differential scanning calorimetry (DSC) was used to measure thermal properties. The measurements were recorded using a Setaram Sensys Evo TG-DSC and PerkinElmer Diamond DSC with a temperature ranges of 0–320 °C, under a scanning rate of 10 °C min^{-1}. Gel permeation chromatography (GPC) analyses were performed to calculate the molecular weight of polymeric precursors. A TOSOH EcoSEC GPC system was used. The system contains a pump with temperature control, a sampler with an automatic system, a RI detector, an oven for the column, a column TSKgel SuperhZ2000, 4.6 mm ID $\times$ 15 cm $\times$ 2 cm, and a purge and degasser unit. The eluent of the system is THF. The flow rate is 1.0 mL min^{-1} at 40 °C. Polystyrene was used as standard to calibrate to refractive index detector. Eco-SEC

Analysis software was used to analyze the data obtained.

2.3. Synthesis of catechol-based main-chain benzoxazine precursor (CTBz)

Catechol (9.08 mmol, 1 g), TTDDA (9.08 mmol, 2 g), and paraformaldehyde (36.3 mmol, 1.09 g) were mixed with $CHCl_3$ and left to reflux for 24 h. Then $CHCl_3$ was totally vaporized with an evaporator. The residual was concentrated. The precipitation was performed in excess diethyl ether (150 mL) by dropwise addition of the concentrated product. After the precipitation process was performed twice, the product was separated by decantation and left to dry in a vacuum oven at room temperature (rt) (yield 65%).

2.4. Synthesis of mPEG-SH

In a 100-mL round flask, poly(ethylene glycol) methyl ether (mPEG) (M_n: 2000 g mol^{-1}) (5 g, 2.5 mmol) was mixed with mercaptopropionic acid (0.8 g, 7.5 mmol) in 50 mL of toluene. H_2SO_4 (two drops) (98%) was added and the resulting mixture was refluxed in a Dean–Stark apparatus until all water was collected in the trap. Then the mixture cooled and the toluene was evaporated in a vacuum pump. The residual was diluted with CH_2Cl_2 (50 mL). After the extraction process with $NaHCO_3$ three or four times, the residue was combined with $MgSO_4$ for drying and filtered. The mixture was concentrated and precipitated with cold diethyl ether. The white product was left to dry in a vacuum oven overnight (yield 75%).

2.5. Synthesis of catechol-poly(ethylene glycol) methyl ether copolymer (CTBz-mPEG)

In a 50-mL flask, mPEG-SH (100 mg, 0.05 mmol, 1 equiv.) and CTBz (400 mg, 0.22 mmol, 5 equiv.) were added to a methanol/THF blend (1:3) (v/v) 4 mL). The flask was left to stir for 24 h at rt. The process was terminated by precipitating in cold methanol after this reaction time and the polymer, CTBz-mPEG, was left to dry in a vacuum oven overnight.

2.6. Film preparation

CTBz and mPEG-SH were mixed for 24 h at rt. The obtained poly(CTBz-mPEG) structure was mixed with $CHCl_3$. The solution was charged into a Teflon mold and left for 6 days to evaporate the solvent. The films were then heated at 100 °C. A brownish cross-linked poly(CTBz-mPEG) film was obtained. A CTBz film was also obtained to get more insight into the effect of the PEG segment.

3. Results and discussion

The CTBz polymer precursor was synthesized using catechol, formaldehyde, and TTDDA as the starting chemicals with the traditional benzoxazine synthesis methodology (Scheme 2). The molar stoichiometric ratio of catechol, diamine, and paraformaldehyde was 1:1:4. Spectral and thermal analyses were used to verify the chemical synthesis of CTBz. As may be seen in the nuclear magnetic resonance spectra (Figure 1), the distinctive peaks at 4.92 and 3.94 ppm were allocated to oxazine ring methylene protons corresponding to O–CH_2–N and Ar–CH_2–N, separately. The proton resonances of the catechol hydroxyls detected at 8.78 ppm completely vanished as expected after the reaction. The aromatic proton resonance of the catechol shifted to the high field, and the integrated intensity decreased as expected. The methylene proton resonances of the diamine functional compounds were detected at 3.48, 2.86, and 1.83 ppm, which corresponded to O–CH_2–C, N–CH_2–C and C–CH_2–C, respectively, and supported the formation of a main-chain-type benzoxazine polymer precursor.

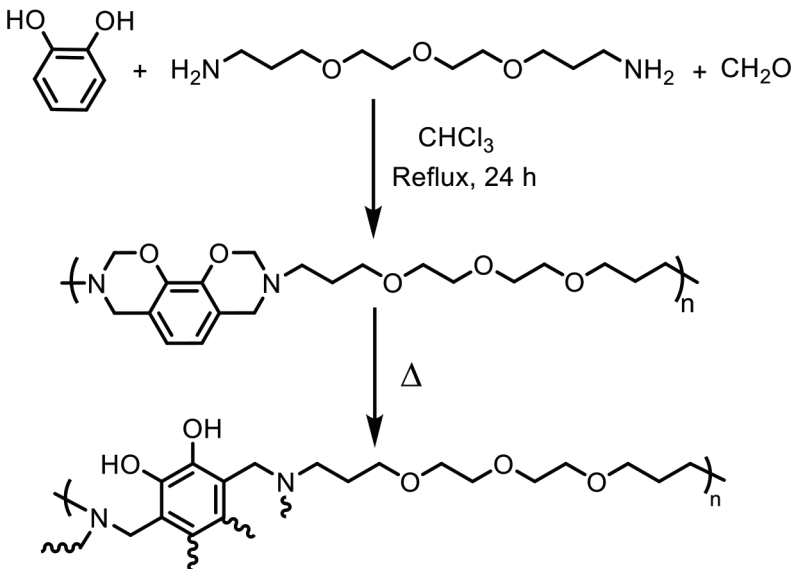

Scheme 2. Synthetic route to CTBz.

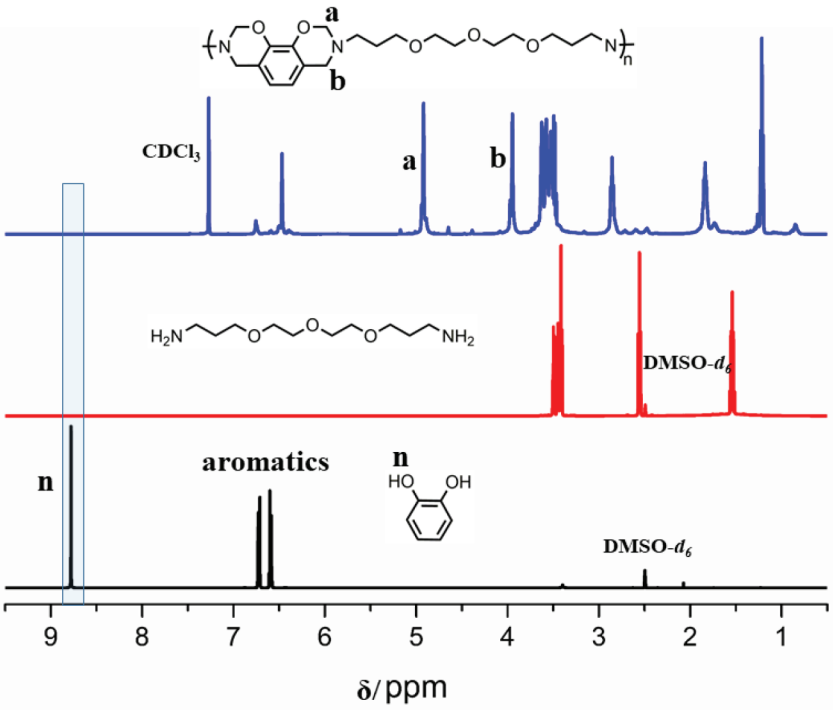

Figure 1. ^{1}H NMR spectra of catechol, TTDDA, and CTBz.

Figure 2 shows the typical bond vibrations of the benzoxazine units including CH_2 vibrations (wagging) at 1490 cm^{-1}, Ar–O–C stretching (asymmetric) at 1105 cm^{-1}, and the oxazine unit's out-of-plane distortion at 995 cm^{-1}. The asymmetric stretching band of the oxazine ring overlapped with C–O–C vibrations of the TTDDA around 1100 cm^{-1}. The catechol hydroxyls' intra- and intermolecular hydrogen bond vibrations were detected between 2935 and 3560 cm^{-1} as a broad band. The disappearance of these bands supports the expected

result structure. The out-of-plane distortion band at 995 cm^{-1} of the oxazine unit and CH_2 wagging vibration band at 1490 cm^{-1} disappeared after ROP by thermal curing, and this was obvious evidence for ring opening of benzoxazine.

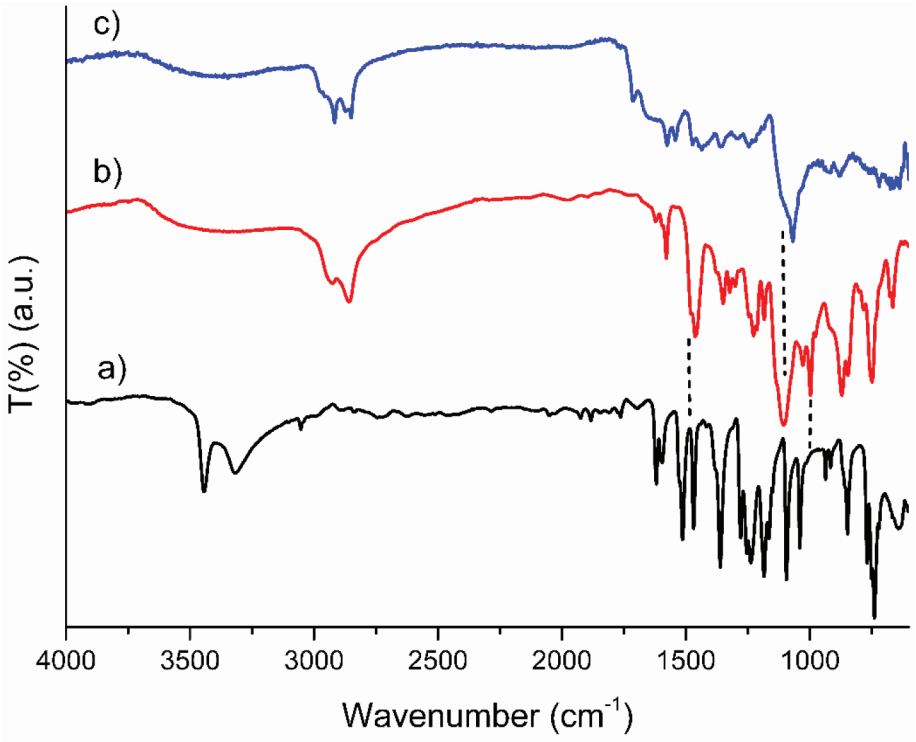

Figure 2. FT-IR spectra of catechol (a), CTBz (b), and cured CTBz (c).

The commonly observed ROP temperature (180–250 °C) of benzoxazines could be decreased by the functional groups including phenolic hydroxyl, alcohol, and carboxylic acid. As may be seen in Figure 3, CTBz exhibited maximum curing at 196 °C. The onset and endset exotherms of CTBz were measured as 187 and 204 °C, respectively. The quantity of the curing exotherm was 217 J/g. The CTBz was thermally cured and then analyzed in DSC to see the effects of heating. The analysis that followed did not exhibit any exothermic peak around the curing temperature range. It verifies the consumption of the oxazine rings during the initial heating course.

As stated in the introduction part, it is important to provide optimal chain mobility conditions and crosslink density to benefit from catechol's superior properties. With this aim, the CTBz polymer was combined with the PEG polymer via a COLBERT reaction. Firstly, mPEG-SH was synthesized from poly(ethylene glycol) methyl ether (mPEG) (M_n: 2000 g mol^{-1}) by Fischer esterification with mercaptopropionic acid in good yield (Scheme 3). PEG was selected to introduce sufficient dynamics to the structure. To access the copolymer structure (poly(CTBz-mPEG)), the synthesized mPEG-SH was reacted with the CTBz. Spectral and thermal analyses were performed to clarify the chemical structure of the poly(CTBz-mPEG). The effect of the PEG segment on the flexibility of the resulting structure was examined. For this, the film was prepared by mixing the CTBz with mPEG-SH in a Teflon mold and by heating at 100 °C. A brownish cross-linked poly(CTBz-mPEG) film was obtained. A CTBz film was also obtained to get more insight into the effect of the PEG segment.

In Figure 4, the ^{1}H NMR spectra of the CTBz and poly(CTBz-mPEG) are overlaid for their soluble parts

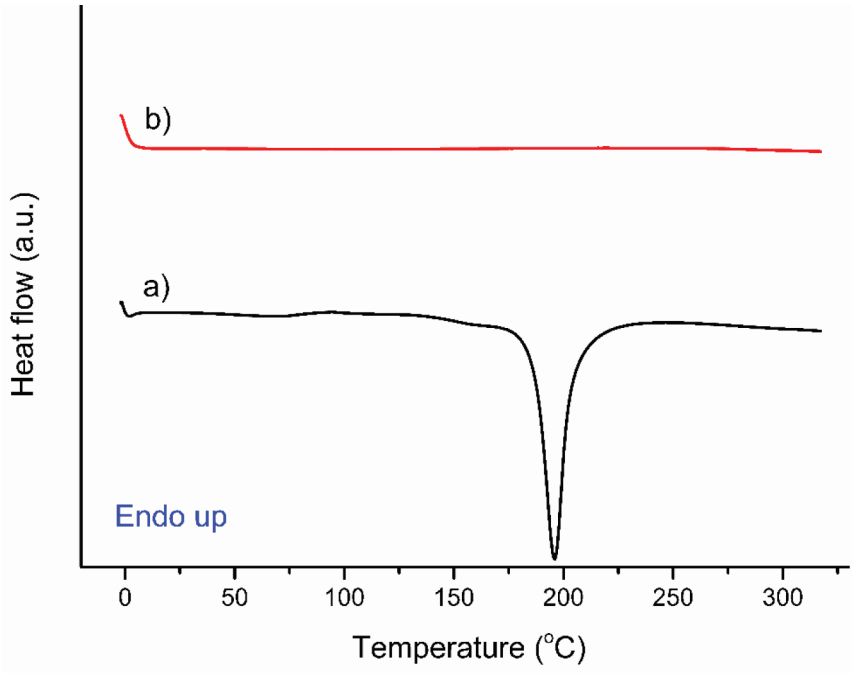

Figure 3. DSC thermograms of CTBz (a) and cured CTBz (b).

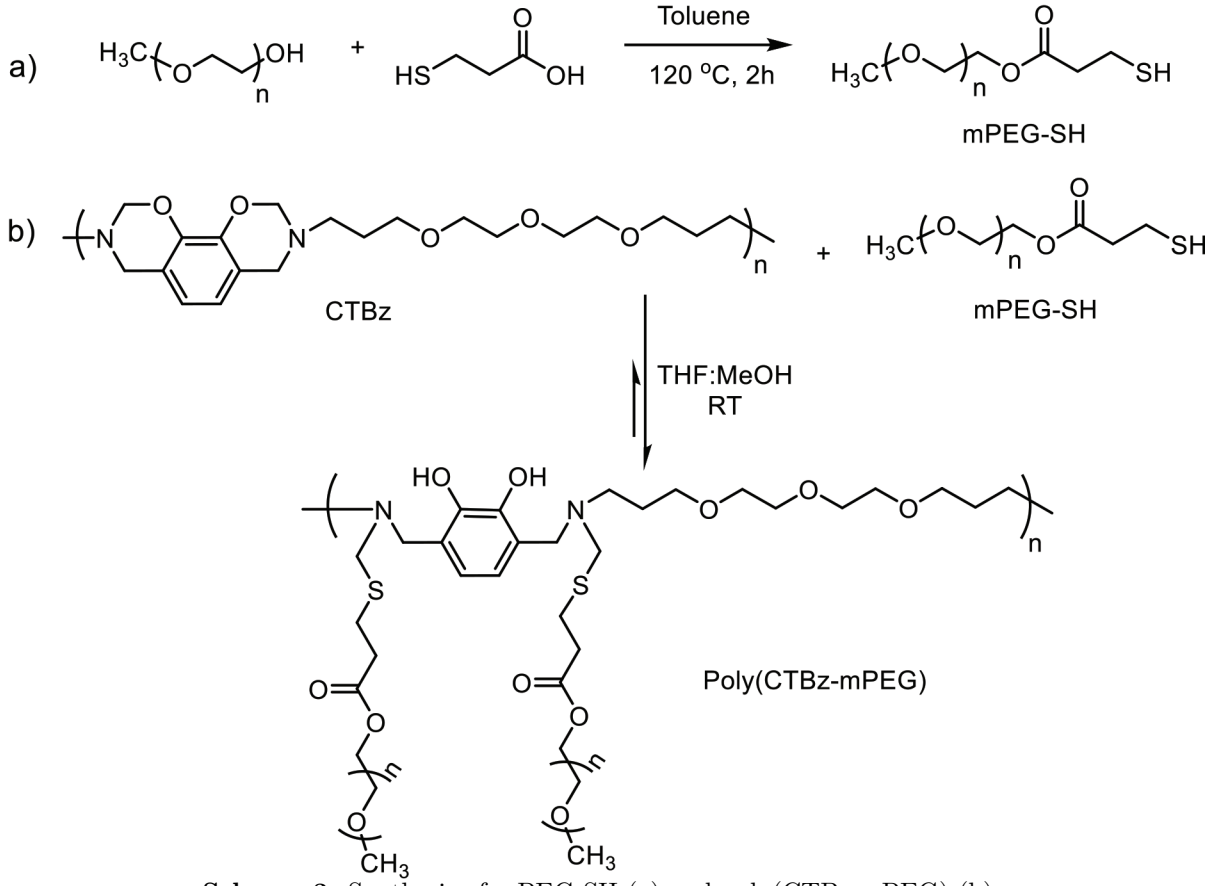

Scheme 3. Synthesis of mPEG-SH (a) and poly(CTBz-mPEG) (b).

in the NMR solvent. The characteristic resonances around 4.92 and 3.94 ppm were allocated to the oxazine ring's methylene protons (O–CH_2–N and Ar–CH_2–N) and were detectable for both structures. The intensity of the –CH_2 proton signals was decreased by the ring-opened oxazine units. The ring-opened and unopened benzoxazine rings were observed in the poly(CTBz-mPEG) structure obtained. The reason for this outcome could be the reversible nature of the mechanism. The resonance shifts of catechol hydroxyl protons placed at 8.78 ppm were observed following the reaction. The corresponding PEG protons were observed between 3.12 and 3.63 ppm.

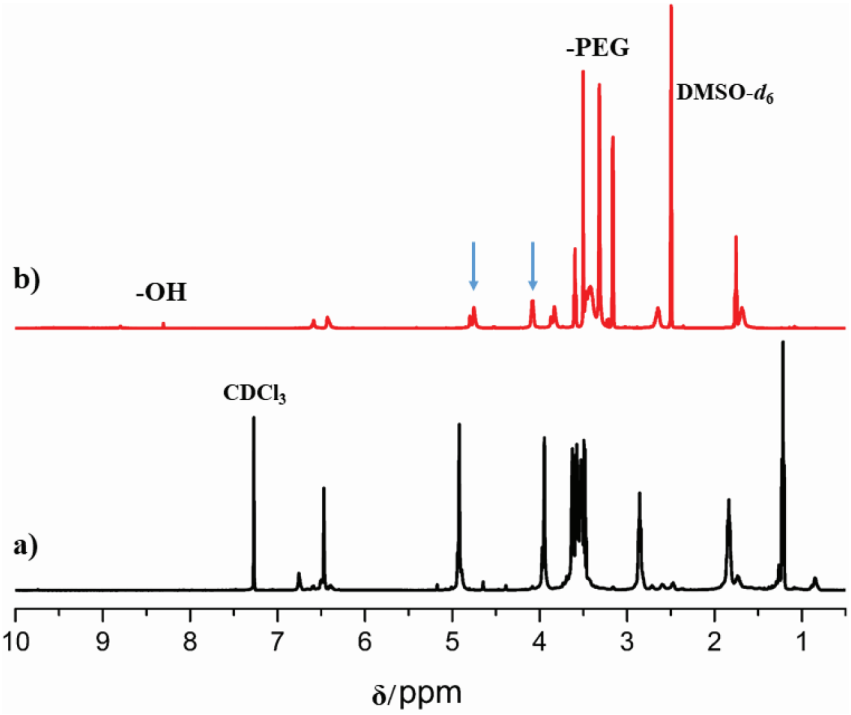

Figure 4. ^{1}H NMR spectra of CTBz (a) and poly(CTBz-mPEG) (b).

The FT-IR spectra of the poly(CTBz-mPEG) are shown in Figure 5. Ester functionality was revealed by the band at 1734 cm^{-1} for the C=O bond. The broad vibration band between 3000 and 3600 cm^{-1} was related to the –OH group of phenols. Additionally, increased band density for the C–O of PEG at around 1100 cm^{-1} was detected for poly(CTBz-mPEG), which demonstrated integration of the PEG segment with the targeted structure.

The high ROP temperatures of benzoxazines should be decreased by structures such as phenolic hydroxyl, alcohol, and carboxylic acid with a reduced exothermic ring-opening temperature in DSC. Therefore, thiol groups should decrease the ROP temperature. The remaining unreacted benzoxazine units in the poly(CTBz-mPEG) were accessible for the subsequent curing process. The ROP took place with heat treatment. As may be seen in Figure 6, the ROP temperature of the poly(CTBz-mPEG) decreased from 196 to 189 °C due to the thiols and formed free phenolic hydroxyls after the COLBERT reaction. The same effect was observed for the onset ROP temperature decreasing from 187 to 177 °C, and these results were compatible with those in the literature (Table 1). The thermal analysis of the copolymer from the DSC thermogram of the poly(CTBz-mPEG) exhibited an endothermic peak at 51 °C indicating the presence of a semicrystalline PEG domain. In such block copolymers, the crystals of PEG segments strongly depend on the molecular weight of the polyether block. In this system,

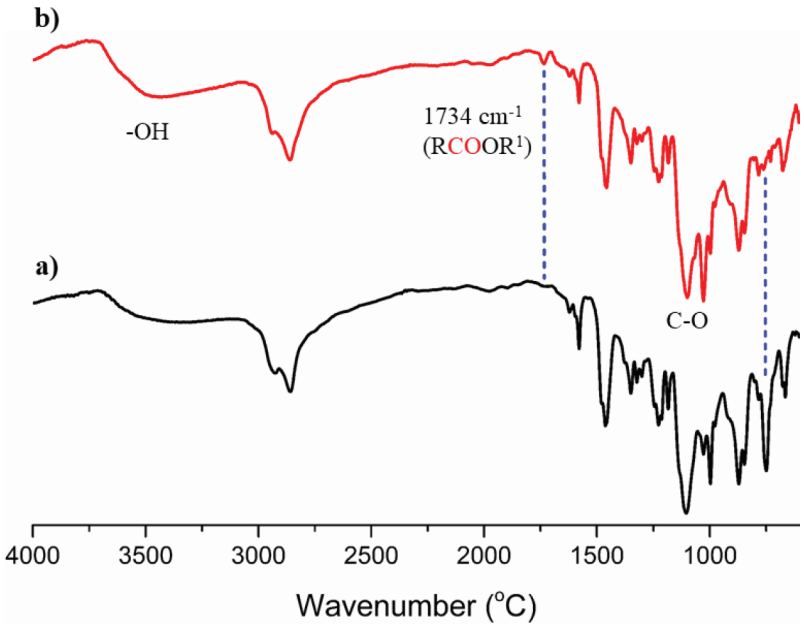

Figure 5. FT-IR spectra of CTBz (a) and poly(CTBz-mPEG) (b).

the block copolymer showed an intense melting transition due to the 2000 g/mol molecular weight PEG segment for the 1st and 2nd heating cycles.

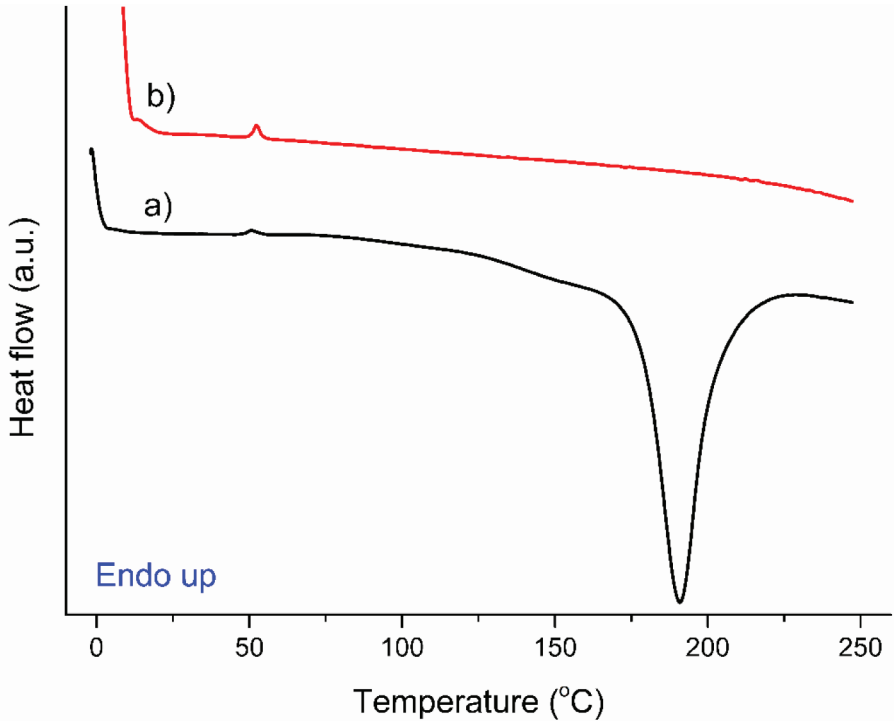

Figure 6. DSC thermographs of poly(CTBz-mPEG) (1st heating) (a) and cured poly(CTBz-mPEG) (2nd heating) (b).

The molecular weights of the CTBz and the poly(CTBz-mPEG) were measured as 1810 Da (M_w/M_n: 1.10) and 4400 Da (M_w/M_n: 1.03), respectively, via GPC analysis. It may be concluded from the GPC

Table 1. DSC[a] characteristics of CTBz and poly(CTBz-mPEG).

Entry	Heating rate (°C/min)	Onset of curing (°C)	Endset of curing (°C)	Maximum curing (°C)	ΔH (J/g)
CTBz	10	187	204	196	–217
Poly(CTBz-mPEG)	10	177	202	189	–181

[a] DSC investigations were performed with a 20 mL min^{-1} N_2 gas atmosphere. The heating rate is 10 °C min^{-1}.

thermograms that each CTBz chain contained nearly 5 catechol and amine monomers. After the COLBERT reaction, the molecular weight (mean number) of CTBz increased as expected due to the PEG segment's attachment. These results were obtained from the soluble part of the CTBz and poly(CTBz-mPEG) in THF. Thus, the molecular weight of the insoluble part of the poly(CTBz-mPEG) should be higher.

Thermogravimetric analysis (TGA) was performed to examine the thermal properties of the PCTBz and poly(CTBz-mPEG). As may be seen in the TGA traces in Figure 7, the cured catechol–benzoxazine polymer PCTBz and poly(CTBz-mPEG) clearly showed high char yields. The raw diamine compound was nearly vaporized at 900 °C and had no char yield. The PCTBz and poly(CTBz-mPEG) displayed char yields of respectively 40% and 43% due to the large amount of benzoxazine unit in the resulting structure (Table 2). These results obviously supported the integration of benzoxazine units and PEG segments into the target material.

Table 2. Thermal stability and char yields of cured PCTBz and poly(CTBz-mPEG) calculated by TGA.

Polymers	$T_{5\%}$ (°C)	$T_{10\%}$ (°C)	T_{max} (°C)	Y_c (%)
PCTBz	271	291	359	40
Poly(CTBz-mPEG)	274	298	365	43

$T_{5\%,\,10\%}$: 5% and 10% weight loss were detected at these temperatures, respectively, T_{max}: Maximum weight loss was detected at this temperature, Y_c: The amount of detected char yields at 900 °C with N_2 atmosphere.

Figure 8 shows a visual demonstration of the films that were prepared. The images a and b correspond to the CTBz film without any heating. The images d and e correspond to the poly(CTBz-mPEG) films in heating conditions of 100 °C for 1 h. The films had sufficient elasticity in both conditions as may be seen in the images. The films became brittle after curing at 200 °C. It may be considered that the high amount of the remaining oxazine units in the resulting structure should have behaved as a crosslinker.

4. Conclusion

Consequently, we revealed that a novel flexible catechol-based benzoxazine film can be obtained simply from polymeric main-chain benzoxazine precursors through the oxazine rings by a COLBERT reaction. The precursors were prepared by the traditional benzoxazine synthesis and Fischer esterification processes. The reaction of the CTBz and mPEG-SH resulted in a benzoxazine-PEG copolymer structure, and it was able to provide

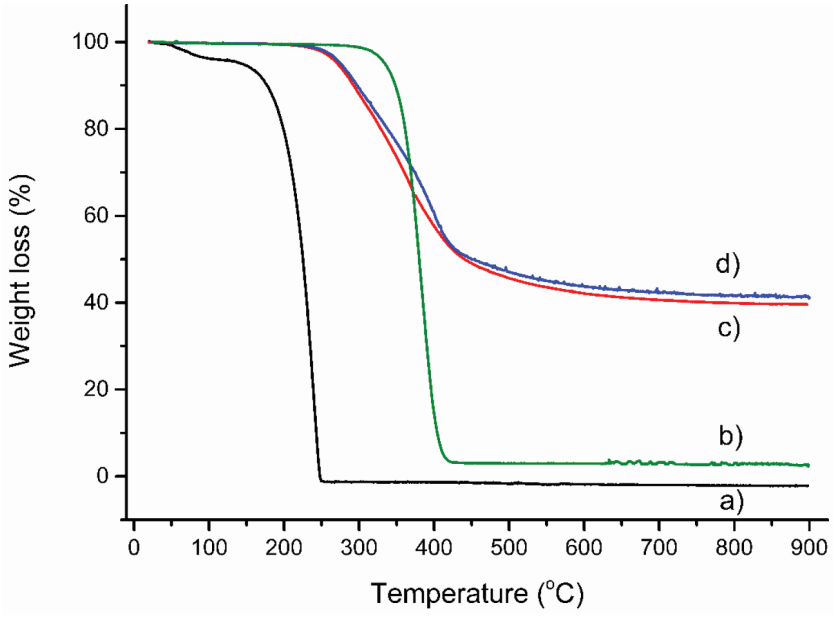

Figure 7. TGA traces of TTDDA (a), mPEG-SH (b), cured CTBz (c), and cured poly(CTBz-mPEG) (d).

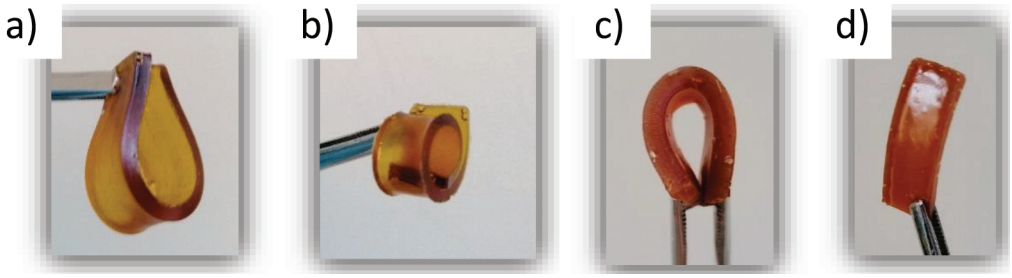

Figure 8. Images of flexible CTBz film (a, b) before heating and poly(CTBz-mPEG) film (c, d) after heating.

flexible films. The obtained films were curable due to the remaining benzoxazine units with a partially low ROP temperature. It may be concluded that benzoxazine precursors might be converted into copolymers using the related benzoxazine and thiol structures via the COLBERT process. The easy and fast reaction environments at ambient conditions and accessibility of broad series of thiol compounds are the main advantages of this approach. The design flexibility and simplicity of benzoxazine precursor synthesis are also further advantages for desired polymer syntheses.

Acknowledgment

We thank the Research Fund of Kırklareli University for its financial support (KLUBAP-129).

References

1. Ghosh NN, Kiskan B, Yagci Y. Polybenzoxazines - new high performance thermosetting resins: synthesis and properties. Progress in Polymer Science 2007; 32 (11): 1344-1391. doi: 10.1016/j.progpolymsci.2007.07.002
2. Yagci Y, Kiskan B, Ghosh NN. Recent advancement on polybenzoxazine - a newly developed high performance thermoset. Journal of Polymer Science Part A: Polymer Chemistry 2009; 47 (21): 5565-5576. doi: 10.1002/pola.23597

3. Arslan M, Kiskan B, Yagci Y. Post-modification of polybutadienes by photoinduced hydrogen abstraction from benzoxazines and their thermally activated curing. Macromolecules 2016; 49 (14): 5026-5032. doi: 10.1021/acs.macromol.6b01329
4. Tasdelen MA, Kiskan B, Yagci Y. Photoinitiated free radical polymerization using benzoxazines as hydrogen donors. Macromolecular Rapid Communications 2006; 27 (18): 1539-1544. doi: 10.1002/marc.200600424
5. Tasdelen MA, Durmaz H. Thermally curable polyoxanorbornene by ring opening metathesis polymerization. Macromolecular Chemistry and Physics 2011; 212 (19): 2121-2126. doi: 10.1002/macp.201100258
6. Demir KD, Tasdelen MA, Uyar T, Kawaguchi AW, Sudo A et al. Synthesis of polybenzoxazine/clay nanocomposites by in situ thermal ring-opening polymerization using intercalated monomer. Journal of Polymer Science Part A: Polymer Chemistry 2011; 49 (19): 4213-4220. doi: 10.1002/pola.24863
7. Taskin OS, Kiskan B, Yagci Y. Polybenzoxazine precursors as self-healing agents for polysulfones. Macromolecules 2013; 46 (22): 8773-8778. doi: 10.1021/ma4019153
8. Sharma P, Kumar D, Roy PK. Microwave-assisted sustainable synthesis of telechelic poly(ethylene glycol)s with benzoxazine end groups. 2016; 1 (21): 6941-6947. doi: 10.1002/slct.201601226
9. Dizman C, Altinkok C, Tasdelen MA. Synthesis of self-curable polysulfone containing pendant benzoxazine units via CuAAC click chemistry. Designed Monomers and Polymers 2017; 20 (1): 293-299. doi: 10.1080/15685551.2016.1257379
10. Trejo-Machin A, Verge P, Puchot L, Quintana R. Phloretic acid as an alternative to the phenolation of aliphatic hydroxyls for the elaboration of polybenzoxazine. Green Chemistry 2017; 19 (21): 5065-5073. doi: 10.1039/C7GC02348K
11. Brown EA, Rider DA. Pegylated polybenzoxazine networks with increased thermal stability from miscible blends of tosylated poly(ethylene glycol) and a benzoxazine monomer. Macromolecules 2017; 50 (17): 6468-6481. doi: 10.1021/acs.macromol.7b01457
12. Van A, Chiou K, Ishida H. Use of renewable resource vanillin for the preparation of benzoxazine resin and reactive monomeric surfactant containing oxazine ring. Polymer 2014; 55 (6): 1443-1451. doi: 10.1016/j.polymer.2014.01.041
13. Sini NK, Bijwe J, Varma IK. Renewable benzoxazine monomer from vanillin: synthesis, characterization, and studies on curing behavior. Journal of Polymer Science Part A: Polymer Chemistry 2014; 52 (1): 7-11. doi: 10.1002/pola.26981
14. Calo E, Maffezzoli A, Mele G, Martina F, Mazzetto SE et al. Synthesis of a novel cardanol-based benzoxazine monomer and environmentally sustainable production of polymers and bio-composites. Green Chemistry 2007; 9 (7): 754-759. doi: 10.1039/b617180j
15. Dayo AQ, Wang AR, Derradji M, Kiran S, Zegaoui A et al. Copolymerization of mono and difunctional benzoxazine monomers with bio-based phthalonitrile monomer: curing behaviour, thermal, and mechanical properties. Reactive & Functional Polymers 2018; 131: 156-163. doi: 10.1016/j.reactfunctpolym.2018.07.022
16. Dumas L, Bonnaud L, Olivier M, Poorteman M, Dubois P. High performance bio-based benzoxazine networks from resorcinol and hydroquinone. European Polymer Journal 2016; 75: 486-494. doi: 10.1016/j.eurpolymj.2016.01.021
17. Thirukumaran P, Shakila A, Muthusamy S. Synthesis and characterization of novel bio-based benzoxazines from eugenol. RSC Advances 2014; 4 (16): 7959-7966. doi: 10.1039/c3ra46582a
18. He Y, Gao S, Lu Z. A mussel-inspired polybenzoxazine containing catechol groups. Polymer 2018; 158: 53-58. doi: https://doi.org/10.1016/j.polymer.2018.10.046
19. Xu H, Lu Z, Zhang G. Synthesis and properties of thermosetting resin based on urushiol. RSC Advances 2012; 2 (7): 2768-2772. doi: 10.1039/C2RA00829G
20. Wang CF, Sun JQ, Liu XD, Sudo A, Endo T. Synthesis and copolymerization of fully bio-based benzoxazines from guaiacol, furfurylamine and stearylamine. Green Chemistry 2012; 14 (10): 2799-2806. doi: 10.1039/c2gc35796h

21. Lou YJ, Zhao ZX, Chen ZW, Dai ZH, Fu FY et al. Processability improvement of a 4-vinlyguiacol derived benzoxazine using reactive diluents. Polymer 2019; 160: 316-324. doi: 10.1016/j.polymer.2018.11.056

22. Liu YL, Chou C I. High performance benzoxazine monomers and polymers containing furan groups. Journal of Polymer Science Part A: Polymer Chemistry 2005; 43 (21): 5267-5282. doi: 10.1002/pola.21023

23. Kotzebue LRV, De Oliveira JR, Da Silva JB, Mazzetto SE, Ishida H et al. development of fully biobased high-performance bis-benzoxazine under environmentally friendly conditions. ACS Sustainable Chemistry & Engineering 2018; 6 (4): 5485-5494. doi: 10.1021/acssuschemeng.8b00340

24. Oliveira JR, Kotzebue LRV, Mazzetto SE, Lomonaco D. Towards bio-based high-performance polybenzoxazines: agro-wastes as starting materials for BPA-free thermosets via efficient microwave-assisted synthesis. European Polymer Journal 2019; 116: 534-544. doi: https://doi.org/10.1016/j.eurpolymj.2019.04.014

25. Dumas L, Bonnaud L, Olivier M, Poorteman M, Dubois P. Chavicol benzoxazine: ultrahigh Tg biobased thermoset with tunable extended network. European Polymer Journal 2016; 81: 337-346. doi: 10.1016/j.eurpolymj.2016.06.018

26. Arslan M. Synthesis and characterization of novel bio-based benzoxazines from gallic acid with latent catalytic characteristics. Reactive and Functional Polymers 2019; 139. doi: 10.1016/j.reactfunctpolym.2019.03.011

27. Gorodisher I, Devoe RJ, Webb RJ. Catalytic opening of lateral benzoxazine rings by thiols. In: Ishida H, Agag T, editors. Handbook of Benzoxazine Resins. Amsterdam, Netherlands: Elsevier, 2011, pp. 211-234.

28. Semerci E, Kiskan B, Yagci Y. Thiol reactive polybenzoxazine precursors: a novel route to functional polymers by thiol-oxazine chemistry. European Polymer Journal 2015; 69: 636-641. doi: 10.1016/j.eurpolymj.2015.02.030

29. Urbaniak T, Soto M, Liebeke M, Koschek K. Insight into the mechanism of reversible ring-opening of 1,3-benzoxazine with thiols. The Journal of Organic Chemistry 2017; 82 (8): 4050-4055. doi: 10.1021/acs.joc.6b02727

30. Oie H, Mori A, Sudo A, Endo T. Polyaddition of bifunctional 1,3-benzoxazine and 2-methylresorcinol. Journal of Polymer Science Part A: Polymer Chemistry 2013; 51 (18): 3867-3872. doi: 10.1002/pola.26784

31. Beyazkilic Z, Kahveci MU, Aydogan B, Kiskan B, Yagci Y. Synthesis of polybenzoxazine precursors using thiols: simultaneous thiol-ene and ring-opening reactions. Journal of Polymer Science Part A: Polymer Chemistry 2012; 50 (19): 4029-4036. doi: 10.1002/pola.26202

32. Bektas S, Kiskan B, Orakdogen N, Yagci Y. Synthesis and properties of organo-gels by thiol-benzoxazine chemistry. Polymer 2015; 75: 44-50. doi: 10.1016/j.polymer.2015.08.026

33. Musa A, Kiskan B, Yagci Y. Thiol-benzoxazine chemistry as a novel Thiol-X reaction for the synthesis of block copolymers. Polymer 2014; 55 (22): 5550-5556. doi: 10.1016/j.polymer.2014.06.076

34. Lowe AB. Thiol-yne 'click'/coupling chemistry and recent applications in polymer and materials synthesis and modification. Polymer 2014; 55 (22): 5517-5549. doi: 10.1016/j.polymer.2014.08.015

35. Ye Q, Zhou F, Liu WM. Bioinspired catecholic chemistry for surface modification. Chemical Society Reviews 2011; 40 (7): 4244-4258. doi: 10.1039/c1cs15026j

36. Sedo J, Saiz-Poseu J, Busque F, Ruiz-Molina D. Catechol-based biomimetic functional materials. Advanced Materials 2013; 25 (5): 653-701. doi: 10.1002/adma.201202343

37. Higginson CJ, Malollari KG, Xu Y, Kelleghan AV, Ricapito NG et al. Bioinspired design provides high-strength benzoxazine structural adhesives. Angewandte Chemie International Edition 2019; 58 (35): 12271-12279. doi: 10.1002/anie.201906008

38. Li L, Li Y, Luo XF, Deng JP, Yang WT. Helical poly(N-propargylamide)s with functional catechol groups: synthesis and adsorption of metal ions in aqueous solution. Reactive & Functional Polymers 2010; 70 (12): 938-943. doi: 10.1016/j.reactfunctpolym.2010.09.006

39. Wang J, Liu CS, Lu X, Yin M. Co-polypeptides of 3,4-dihydroxyphenylalanine and L-lysine to mimic marine adhesive protein. Biomaterials 2007; 28 (23): 3456-3468. doi: 10.1016/j.biomaterials.2007.04.009

40. Lee BP, Chao CY, Nunalee FN, Motan E, Shull KR et al. Rapid gel formation and adhesion in photocurable and biodegradable block copolymers with high DOPA content. Macromolecules 2006; 39 (5): 1740-1748. doi: 10.1021/ma0518959

41. Yuan SJ, Wan D, Liang B, Pehkonen SO, Ting YP et al. Lysozyme-coupled poly(poly(ethylene glycol) methacrylate)-stainless steel hybrids and their antifouling and antibacterial surfaces. Langmuir 2011; 27 (6): 2761-2774. doi: 10.1021/la104442f

42. Wang JJ, Tahir MN, Kappl M, Tremel W, Metz N et al. Influence of binding-site density in wet bioadhesion. Advanced Materials 2008; 20 (20): 3872-3876. doi: 10.1002/adma.200801140

43. Shao H, Stewart RJ. Biomimetic underwater adhesives with environmentally triggered setting mechanisms. Advanced Materials 2010; 22 (6): 729-733. doi: 10.1002/adma.200902380

44. White JD, Wilker JJ. Underwater bonding with charged polymer mimics of marine mussel adhesive proteins. Macromolecules 2011; 44 (13): 5085-5088. doi: 10.1021/ma201044x

45. Chung HY, Glass P, Pothen JM, Sitti M, Washburn NR. Enhanced adhesion of dopamine methacrylamide elastomers via viscoelasticity tuning. Biomacromolecules 2011; 12 (2): 342-347. doi: 10.1021/bm101076e

46. Ryu JH, Lee Y, Kong WH, Kim TG, Park TG et al. Catechol-functionalized chitosan/pluronic hydrogels for tissue adhesives and hemostatic materials. Biomacromolecules 2011; 12 (7): 2653-2659. doi: 10.1021/bm200464x

47. Adkins CT, Dobish JN, Brown CS, Mayrsohn B, Hamilton SK et al. High relaxivity MRI imaging reagents from bimodal star polymers. Polymer Chemistry 2012; 3 (2): 390-398. doi: 10.1039/c1py00474c

48. Saxer S, Portmann C, Tosatti S, Gademann K, Zurcher S et al. Surface assembly of catechol-functionalized poly (l-lysine)-graft-poly (ethylene glycol) copolymer on titanium exploiting combined electrostatically driven self-organization and biomimetic strong adhesion. Macromolecules 2009; 43 (2): 1050-1060. doi: 10.1021/ma9020664

49. Han H, Wu JF, Avery CW, Mizutani M, Jiang XM et al. Immobilization of amphiphilic polycations by catechol functionality for antimicrobial coatings. Langmuir 2011; 27 (7): 4010-4019. doi: 10.1021/la1046904